Morphological and adhesive properties of polypyrrole films

synthesized by sonoelectrochemical technique

Jérôme Dejeu[1], Abdeslam Et Taouil[2], Patrick Rougeot[1], Sophie Lakard[2], Fabrice Lallemand[2],

Boris Lakard[2],*

1 Institut FEMTO-ST, CNRS-UFC-ENSMM-UTBM, AS2M Department, 24 rue Alain Savary, 25000 Besançon, France.

2 Institut UTINAM, UMR CNRS 6123, University of Franche-Comté, 16 route de Gray, 25030 Besançon Cedex, France.

Abstract

This paper presents sonochemically deposited polypyrrole films and their characteristics of adhesion on substrate with related to the surface roughness and morphology by comparing to the conventional films deposited electrochemically. In particular, the use of high frequency sonication (500 kHz) for sonoelectrochemical deposition of polypyrrole was reported for the first time. Chronocoulometry was used to electrosynthesize polypyrrole films on Si substrates of different thicknesses in order to determine the influence of the polymer thickness on its rugosity, its morphology and its adhesion force properties. The effects of high frequency sonication on the electropolymerized thin film's properties were investigated using Scanning Electron Microscopy and mechanical probe scanning showing that sonication led to surfaces having a smaller roughness and a better homogeneity than non sonicated ones. The adhesion force properties of polypyrrole films were also studied by means of force-distance curves obtained by Atomic Force Microscopy. For polymer films obtained in the absence of sonication, the measured adhesion forces decreased when the polymer thickness increased. On

the contrary, for polymer films obtained under sonication, the adhesion of the films decreased when the polymer thickness decreased.

* Corresponding author. Tel.: +33 3 81 66 62 95. Fax: +33 3 81 66 64 38.

E-mail address: boris.lakard@univ-fcomte.fr (B. Lakard).

1. Introduction

Since polyacetylene was shown to have high electrical conductivities when properly doped [1,2], π-conjugated organic polymers have been studied extensively from both fundamental and practical points of view. Indeed, these conducting polymers can be used for many various applications including: energy storage and batteries [3-5], field effect transistors [6,7], electrochromic devices [8,9], protection against corrosion [10-12], sensing of liquids [13-18], gas [19-23] and biomolecules [24-28], separation of molecules by polymeric membranes [29,30], electrocatalysis [31,32], development of solar cells [33,34] and light-emitting diodes [35,36]…

Among all the conducting polymers, polypyrrole is one of the most studied for its high electronic conductivity, good stability in air and aqueous media and ease of preparation by electrochemical polymerization. However, the electropolymerized films properties of electropolymerized films are strongly influenced by the parameters chosen for the electrosynthesis: solvent [15,37-39], temperature [40,41], potential or current density [42,43], monomer concentration [44,45], nature of dopant [46-49] and thickness [15,49].

It must also be noticed that several techniques have been used to modify and improve the polymer's properties such as the use of a magnetic [50] or centrifugation fields [51] during electropolymerization. In order to modify and improve polymer film properties, an original technique consists in applying an sonication to the electrolyte solution during the electrochemical deposition of polymer films. This technique has already showed interesting effects on electroorganic processes by playing a role in the electropolymerization of aniline for example [52], as well as by modifying the properties of electrodeposited polymer films through the microagitation and the cavitation phenomena that it generates in liquid media [53,54]. Indeed, sonoelectrochemical procedure provides higher mechanical resistance as well as electrical conductivity as the film characteristics as compared to the film without sonication, as shown in previous works using 20 kHz frequency sonication [54]. On the contrary, at lower frequencies, cavitation phenomena are very violent and cavitation bubbles can implode so violently that this can lead to partial destruction of the electrodeposited polymer film [55] which is definitely unwanted.

In the area for micromanipulation research, the surface modification of micromanipulator is one of the large issues to improve the catching and releasing functionality precisely. Modification of the adhesive characteristics of the manipulator surface with functional polymers is one of the important approaches to resolve the problem. That is why we want to test the ability of sonicated polypyrrole films to functionalize manipulator surface to improve its adhesive properties.

Considering the fact that at high frequencies the behaviour of cavitation bubbles is completely different and the destructive effect of sonication towards the surfaces is reduced compared to at low frequencies, and due to possible deposition of polypyrrole with a high frequency sonication, we use 500kHz sonication for sonoelectrochemical PPy deposition. This sonication overcomes the problem to destroy the PPy film electrodeposited on substrate under

3

20 kHz sonication as generally reported in the literature [54]. The knowledge of the adhesion force is thus essential to enable the advent of reliable micromanipulation techniques. Current approaches are based on experimental measurements performed with atomic force microscope [56,57,58-60], interferometric surface force apparatus [61,62], measurement platform utilizing the contact mechanics theory of Johnson, Kendall, and Roberts [63].

Consequently, in the present work, the effects of polymer thickness and high frequency sonication (500 kHz) on the electropolymerized polypyrrole (PPy) films were studied. Coulometric techniques were used to deeply study PPy films. Important film parameters such as thickness, roughness, morphology and adhesion were explored to observe the effects of sonication. Thus, the determination of the properties of the polymer films allowed us to evaluate the possibility to use them for applications in micromanipulation.

2. Experimental details

2.1. Materials

Pyrrole (ACROS, article 15771 1000, 99% pure) was distilled under reduced pressure before use. Lithium perchlorate $LiClO_4$ (Acros, $\geq$ 99%, 13453-78-6) was used as received without further purification. De-ionized water (solvent) was distilled twice before use (Milli-Q, resistivity 18 MΩ.cm). The substrates used for polymer deposition were 1 0 0-oriented standard 3'' type Si wafers (thickness: 380 μm, p type, dopant: B, resistivity: 0.015 Ω.cm, from Institute of Electronic Materials Technology).

2.2. Electrochemistry

A PGZ-301 potentiostat was employed. The three-electrode setup used consisted of a saturated calomel reference electrode (SCE), a platinum counter-electrode and a Si working

4

electrode (1 cm^2). For sonoelectrochemical experiments, a reactor filled with 700 mL of electrolyte solution is used. The working electrode is immersed in the electrolyte solution and located in front of the ultrasonic transducer (Fig.1). Lithium perchlorate is used as the electrolytic salt. The solvent is water and the concentrations for the studied solution are: 0.1 M in pyrrole and 0.1 M in LiClO$_4$. The electrochemical polymerization of PPy films was done, by applying a potential of 1.2 V/SCE, using chronocoulometry technique. The solutions were kept under an argon flow during the experiments.
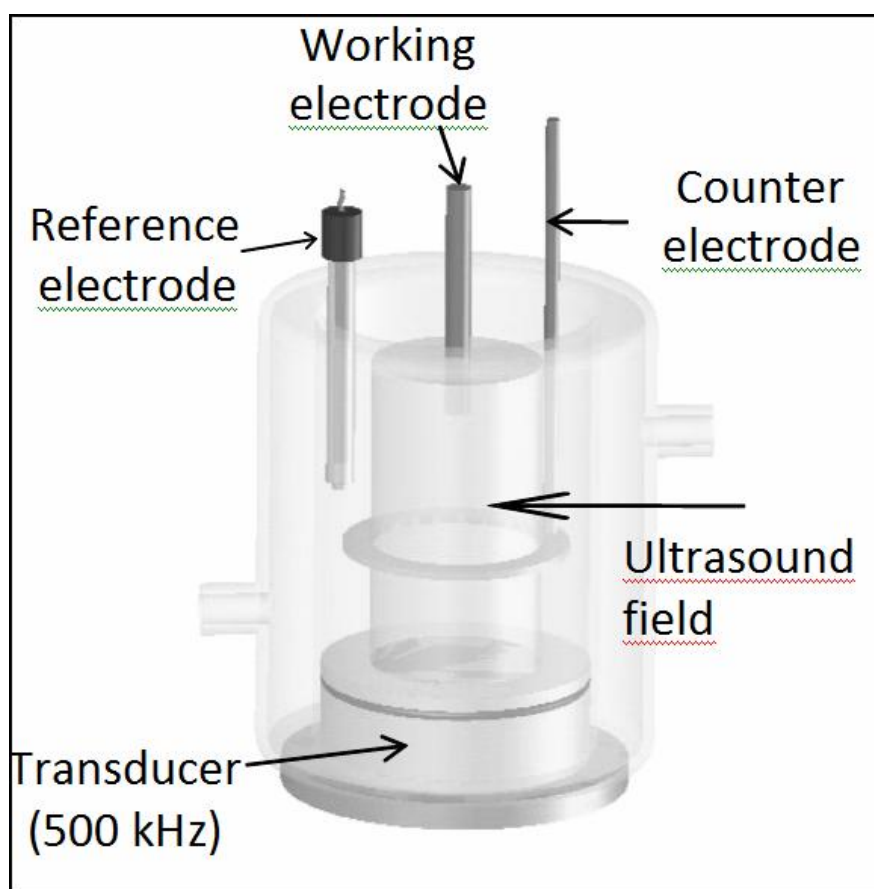
Fig. 1. Scheme of the sonoreactor equipment.

2.3. Sonochemistry

All experiments were performed at a constant ultrasonic frequency of 500 kHz, in a cell filled with 700 ml bath. Sonication is produced parallel to the liquid surface, face to face with the working electrode surface (Fig.1). The circular transducers consist of a piezoelectric ceramic

fixed on a circular plate (56 mm) made of glass. The multifrequency generator is supplied by Electronic Service (St. Alban Leysse, France). An electronic circuit consisting of a variable inductance and capacitor allows the adjustment between the generator impedance and the strongly capacitive transducer impedance.

The sonoreactor was characterized using calorimetric characterization. In this aim, it was filled with distilled water (700 ml) and the ultrasound generator was switched on at an electrical power of 25 W. Thus, the absorbed acoustic power, P_{ac} was calculated using:

$P_{ac} = m.Cp.(dT/dt)$.

where m is the mass of water (kg), C_p the specific heat capacity of water (4180 J kg^{-1} K^{-1}) and (dT/dt) is the temperature rise per second (K s^{-1}). This transmitted acoustic power P_{ac} was found to be equal to 7.8 W.

This characterization was completed by sonochemiluminescence observations. Indeed, acoustic distribution is not homogeneous along the cylindrical sonoreactor [64], and the observation is possible with the help of luminol oxidation. This technique is based on the creation of radicals in the solution due to ultrasound wave propagation. Luminol becomes luminescent in the presence of radical species, which indicates ultrasound activity. The intensity of this activity increases with the intensity of luminescence. It is worth noticing that pictures of light distribution in a horizontal flat transducer are distorted by reflections and/or refractions of the light on the walls of the reactor, which is cylindrical in shape. However the vertical distribution display remains unaffected and it is important to see that ultrasound activity is the most concentrated at the interface solution/air. The working electrode surface is thus placed at this location to take benefit as much as possible from ultrasound activity.

2.4. Surface characterization

X-ray Photoelectron Spectroscopy (XPS, Thermo VG spectrometer) was used to determine elemental composition and to determine the oxidation state of elements. All spectra were recorded at a 45° take-off angle, relative to the substrate with a spectrometer using monochromatized Al Kα radiation (1486.6 eV). The binding energies of the core-levels were calibrated against the C1s binding energy set at 285.0 eV, an energy characteristic of alkyl moieties. The peaks were analyzed using mixed Gaussian-Lorentzian curves (80% of Gaussian character).

The roughness of the polymer films was determined by stylus-based mechanical probe profiler (Alpha-Step IQ, KLA Tencor). Both average roughness (R_a) and peak to peak roughness (R_q) were estimated on a scan length of 1000 µm at a scan speed of 20 µm/s.

Polymer morphologies examinations were performed using a high-resolution scanning electron microscope. Once synthesized and dried, polymer samples were examined in a LEO microscope (Scanning Electron Microscopy LEO stereoscan 440, manufactured by Zeiss–Leica, Köln, Germany) with a electron beam energy of 15 keV.

2.5. Adhesion

The sample characterization was performed with a commercial atomic force microscope (stand-alone SMENA scanning probe microscope NT-MDT, Russian). The experiments were done under controlled environment with a laminar flow (humidity 30 % and 25°C). The forces measurement performed on this Atomic Force Microscope (AFM) was done in the "Nanorol platform" whose aim is to measure the micromanipulation nanoforce and which is based on the measurement of the AFM cantilever deformation with a laser deflection sensor. The Si rectangular AFM cantilever, whose stiffness is 0.3 N/m, was fixed and the substrate moved vertically. These work application objectives are to improve reliability of micro-object manipulation, so interactions have been studied between a micrometric sphere and a plane.

Measurements were in fact performed with a cantilever where a borosilicate sphere (r = 5 μm radius) was glued on the free extremity and below this one (company Novascan Technologies, Ames, USA). Ten measurements were done at different points on the same sample with a driving speed of 1 μm/s. Figure 2 is a typical distance-force curve that allows to measure an attractive force (pull-in force) when the sphere is coming close to the substrate (near -20 nN). Thus, Fig. 2 shows a pull-off force which represents the adhesion between the borosilicate sphere on the tip AFM cantilever and the substrate. In this example, the pull-off force is reaching - 1.1 μN.
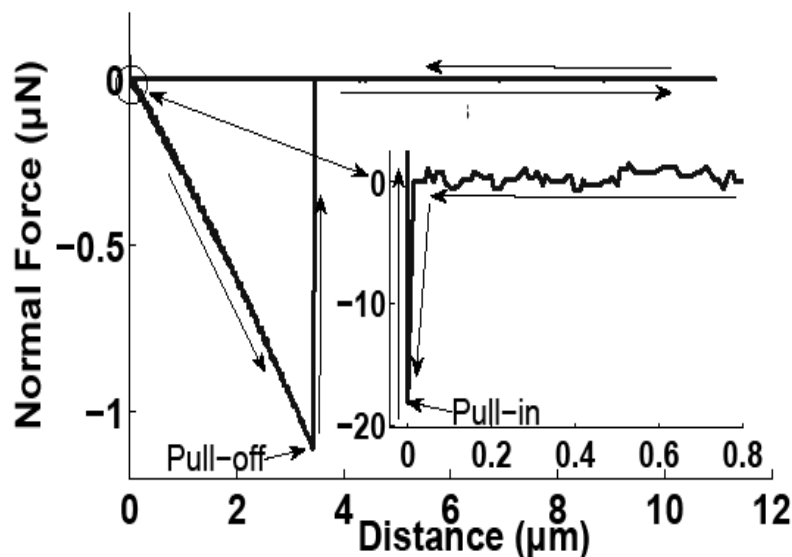
Fig. 2. Attractive and adhesive typical force-distance curves between substrate and cantilever (spring constant: 0.3 N/m).

3. Results and discussion

3.1. (Sono)electrochemical synthesis of polypyrrole films

Polypyrrole films were synthesized, at a fixed potential of 1.2 V/SCE, from aqueous solutions containing 0.1 M pyrrole and 0.1 M LiClO$_4$ on Si substrates. Chronocoulometry (Fig. 3) was used to synthesize the polymer films since this technique allows to determine the charge quantity brought to the electrode in order to control the amount of deposited polymer and the

thickness of the deposited films. To study the effects of high frequency sonication on the electrochemical behaviour of PPy and on the polymer thickness, some PPy films were elaborated under sonication when others were prepared without sonication. Thus, ten films grown at different charge quantity have been studied: 5 were obtained without sonication and 5 with 500 kHz frequency irradiation. The chosen charge densities for the electrosyntheses were 50.1 mC.cm^{-2}, 145.5 mC.cm^{-2}, 243.2 mC.cm^{-2}, 486.4 mC.cm^{-2} and 1459.1 mC.cm^{-2}. More, the chronocoulometry curves (Fig. 3) show that under sonication, the wanted charge quantity is reached much faster than in silent conditions. The improvement of the mass transfer under sonication can be explained by the propagation of the mechanical vibration that creates a global convection within the liquid medium due to the energy losses, which increases mass transfer of the monomers in solution to the electrode. Moreover close to an interface, the collapse of cavitation bubbles becomes asymmetric and the generated micro-jets enhance mass transfer to the electrode surface, allowing its activation by impingement. The monomers are thus brought to the electrode interface more efficiently and a higher current density and better electropolymerization are obtained [65].
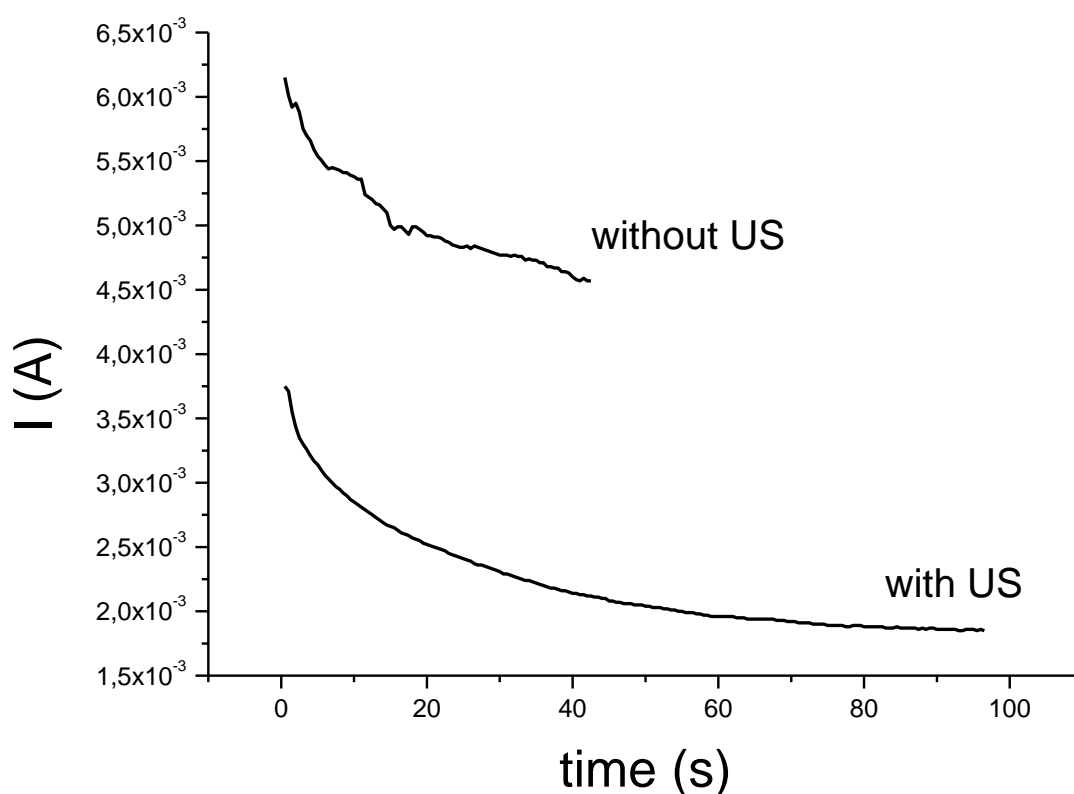
Fig. 3. Chronocoulometry curve of PPy electrosynthesis from an aqueous solution containing 0.1 M pyrrole and 0.1M LiClO$_4$ with and without ultrasonic irradiation. Fixed potential: 1.2 V/SCE, applied charge density: 486.4 mC.cm^{-2}.

3.2. Polypyrrole film thickness

Since the thickness of polymer films can influence their adhesion properties [15,49]. To obtain polypyrrole films of different thickness, the electrical charge associated with pyrrole oxidation was varied using chronocoulometry synthesis technique. To correlate polypyrrole thickness and electrical charge, we used Faraday's law assuming 100 % current efficiency for polypyrrole formation: $x = qM / \rho AzF$ where x is the film thickness, q is the electrical charge associated with polypyrrole formation, M is the molar mass of the polymer, F is the Faraday constant, A is the area of the working surface, ρ is the density of the polymer and z is the number of electrons involved which is in this case of 2.25 [66,67]. The nominal density for

polypyrrole films (ρ) was taken as 1.5 g.cm^{-3} [68,69]. This considered, the required charge density to grow a film with an average thickness of 0.1 μm is 48.5 mC.cm^{-2}. Thus, Table 1 presents the mean film thickness of polypyrrole (x) estimated from electrical charge density (Q) associated with pyrrole oxidation by application of Faraday's law.

electrical charge density (mC.cm^{-2})	Thickness x of the PPy film
50.1	x = 0.1 μm
145.5	x = 0.3 μm
243.2	x = 0.5 μm
486.4	x = 1.0 μm
1459.1	x = 3.0 μm

Table 1: Thicknesses (x) of polypyrrole films as a function of electrical charge density (Q) associated with pyrrole oxidation.

3.3. Characterization of the polypyrrole films

3.3.a. Spectroscopic characterization

Fig. 4a shows the XPS of the 3.0 μm sonicated polypyrrole film deposited onto a Si surface from the oxidation of an aqueous solution containing pyrrole and LiClO$_4$ since this technique is widely used to control the elemental composition of a solid film. The XPS analyses confirm the presence of PPy, incorporating ClO$_4^-$ doping agents, on the platinum surfaces. Indeed, XPS spectra of polymer samples reveal the presence of C, N, O, Cl, Pt for all polymers. Thus, C1s signal (Fig. 4b) can be fitted by five different carbon species at 284.0, 285.0, 286.3, 287.6

11

and 289.1 eV. The two components at the lowest binding energy relevant to β and α carbon

atoms, respectively, revealed the first interesting finding.

In fact, the comparison of these two carbon atoms areas showed that, following overoxidation,

the β carbons in the film were less abundant than the α ones. This indicates, that the β

positions were the ones involved in the polymer functionalization. The third peak at 286.3 eV

is attributed to carbons of the polymer C-N or C-N$^+$; the fourth one at 287.6 eV to C-N$^+$

carbons and the peak much weaker at 289.1 eV to carbonyl C=O groups. The appearance of a

C=O component may be associated with the overoxidation of PPy at the β carbon site in the

pyrrole rings. The N1s spectra (Fig. 4c) indicate the presence of four peaks in the case of PPy.

It contains a main signal at 399.6 eV which is characteristic of pyrrolylium nitrogens (-NH-

structure) and a high BE tail (BE = 400.7 and 402.3 eV) attributable to the positively charged

nitrogen (-NH$^+$ (polaron) and =NH$^+$ (bipolaron)). The spectra also show a small contribution

at 397.3 eV that we associate with =N-structure. Fig. 4d represents the Cl2p core-level XPS

spectrum at 208.3 eV binding energy due to the perchlorate anions present in the film as a

doping agent. Consequently, these XPS spectra confirm that polypyrrole films incorporating

ClO$_4^-$ doping agents are obtained from the oxidation of pyrrole.

(a)

(b)

(c)

(d)
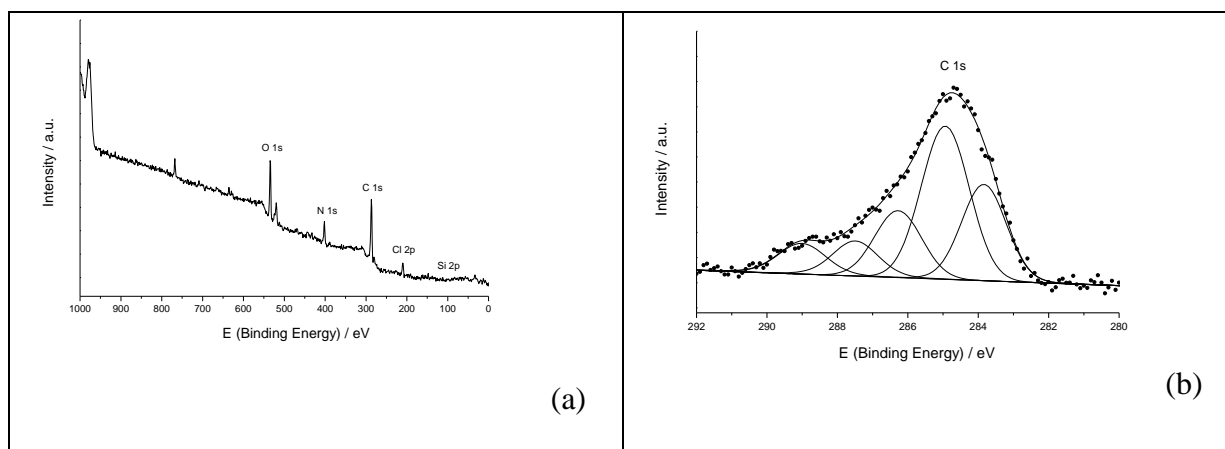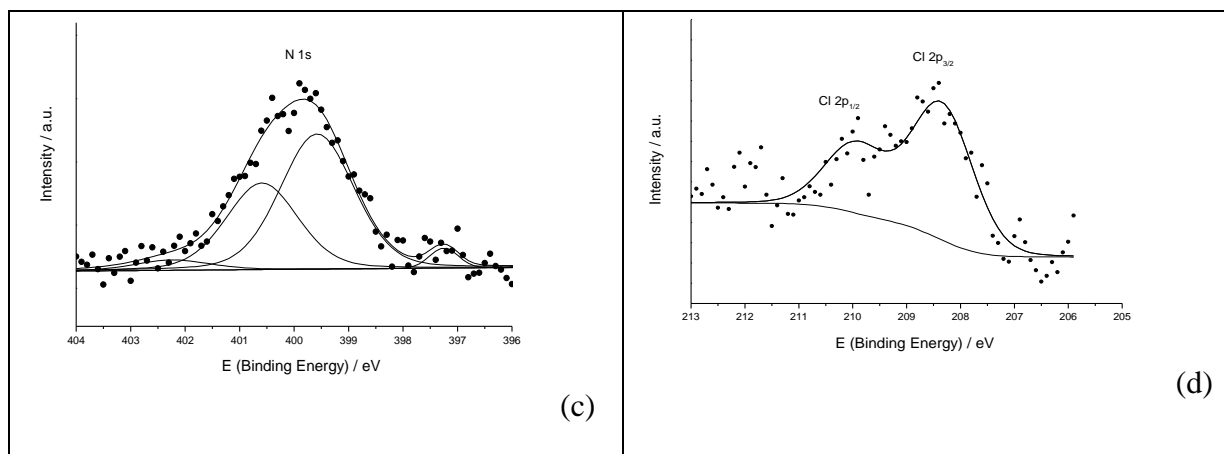
Fig. 4. Survey-scan XPS of polypyrrole films electrosynthesized onto silicon surfaces by oxidation of an aqueous solution of pyrrole and LiClO$_4$ (a). (b) C 1s (c) N 1s (d) Cl 2p XPS spectra of the same polypyrrole film.

3.3.b. Surface morphology

Fig. 5 shows SEM micrographs of PPy films obtained with and without sonication and having a thickness of 0.1 µm and 3 µm. In all cases (Fig. 5), the same squared structure is observed. Nevertheless, the film obtained under sonication appears to have a denser and less squared surface structure. This can be linked to the asymmetric collapse of cavitation bubbles, which lead to activation of the surface by impingement, and certainly therefore to a multiplication of nuclei sites. However, it seems necessary to do roughness measurements to confirm that sonicated PPy films are more homogeneous and have a smaller roughness than non sonicated PPy films.

(a)

(c)

13
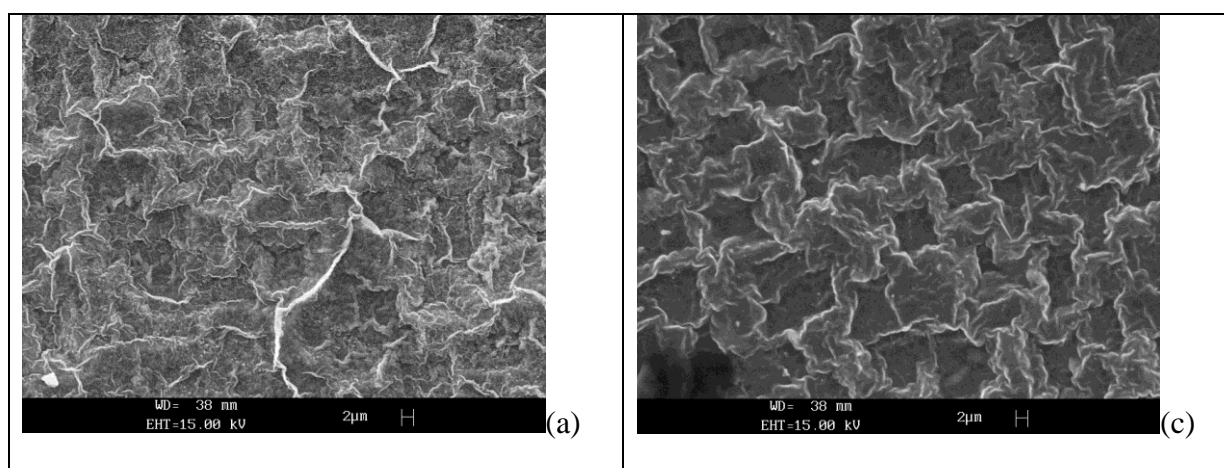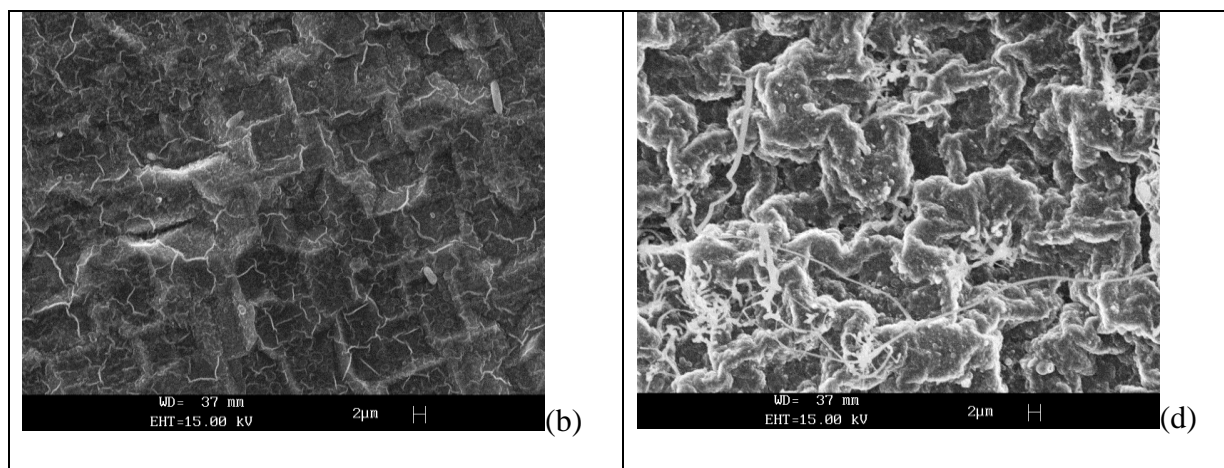
Fig. 5. SEM images of PPy films elaborated under silent conditions (a: 0.1 µm, b: 3 µm) and under ultrasounds (c: 0.1 µm, d: 3 µm).

3.3.c. Polypyrrole film roughness

To understand the values of the adhesion measurements obtained in the next section, it is useful to determine the roughness of each polymer film to correlate the roughness and the adhesion of the polymer films. The Si substrate and the different polypyrrole films roughnesses were investigated using a stylus-based mechanical probe profiler (Table 2). These measurements show that the roughness of PPy films obtained without sonication increases when the thickness increases. However, the average roughness of the three thinnest films are not very different and close to 0.5 µm when the roughness of the two thickest film is far more important (> 1.5 µm). The same trend is observed for PPy films obtained with sonication since the thin films have a roughness close to 0.4 − 0.6 µm when the thickest coatings have average roughness comprises between 0.8 and 1.3 µm. It is also important to note that sonicated PPy films have a smaller roughness than non sonicated ones, indicating that the sonication leads to more homogeneous and smoother surfaces whatever the film thickness.

14

Thickness of the PPy film	Without ultrasonic irradiation	With ultrasonic irradiation
3.0 µm	R_a = 2.370 µm R_q = 2.757 µm	R_a = 1.293 µm R_q = 1.584 µm
1.0 µm	R_a = 1.656 µm R_q = 2.044 µm	R_a = 0.809 µm R_q = 0.943 µm
0.5 µm	R_a = 0.523 µm R_q = 0.628 µm	R_a = 0.444 µm R_q = 0.561 µm
0.3 µm	R_a = 0.502 µm R_q = 0.613 µm	R_a = 0.440 µm R_q = 0.538 µm
0.1 µm	R_a = 0.473 µm R_q = 0.564 µm	R_a = 0.433 µm R_q = 0.537 µm

Table 2: Average roughness (R_a) and peak to peak roughness (R_q) of polypyrrole films as a function of their thickness. For uncoated Si substrate: R_a= 0.392 µm and R_q= 0.504 µm

3.4. Polypyrrole films adhesion properties

The adhesion force, so called pull-off force, was measured for all polymer coatings versus their thickness and their electrodeposition condition (with or without sonication). The experimental curves are presented Figure 6. Figure 6a indicates a weak influence of the thickness on the pull-off force without sonication since the pull-off force evolves from 32 to 44 nN. The use of sonication decreases the adhesion force to 12 nN for the smallest thickness (0.1 µm). The average value of the different measurements at different thicknesses and electrodeposition condition are summarized in Table 3. From this table, it can also be noted that the adhesion force measured between the cantilever and the polyppyrole film was very inferior to that measured between the free polymer substrate and the cantilever (near hundred times less than for 0.1 µm sonicated PPy film). Consequently, when applied to micromanipulation, the PPy film electrodeposited under sonication on the gripper end-effector

could be an interesting coating to decrease drastically the adhesion force. The unique problem is the film grip on the Si wafer. Indeed, sometimes during the cantilever retract after contact with PPy film, a polymer film fragment was attached on the sphere extremity. The film grip must be improved before the micromanipulation task test on robot.
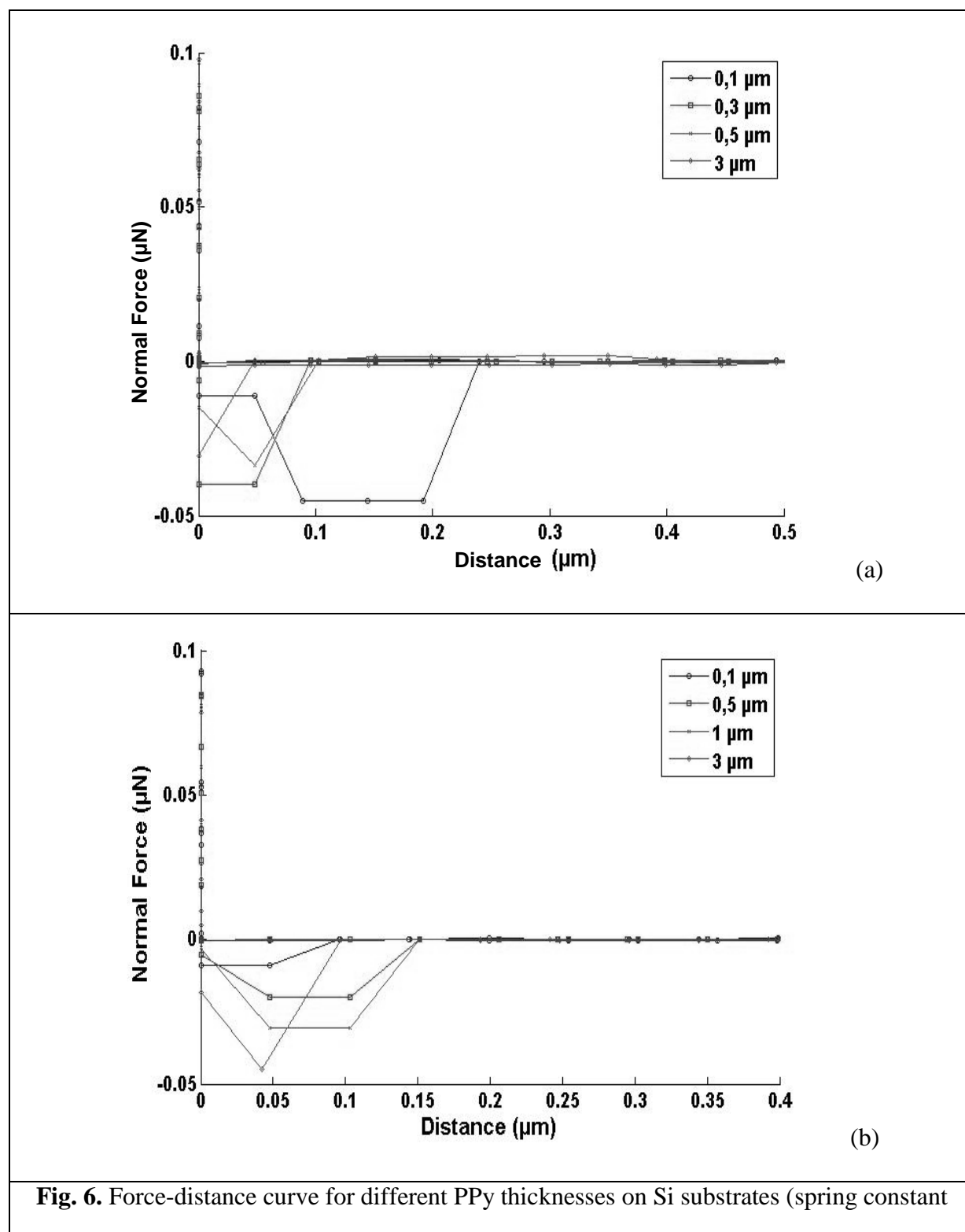
Fig. 6. Force-distance curve for different PPy thicknesses on Si substrates (spring constant

16

0.3 N/m). a: without, b: with ultrasonic irradiation.

PPy thickness	Without US	With US
3 µm	32 nN	41 nN
1 µm	34 nN	36 nN
0,5 µm	37 nN	18 nN
0,3 µm	41 nN	16 nN
0,1 µm	44 nN	12 nN
Uncoated Si	1 µN	

Table 3: Influence of the PPy film thickness on the Pull-off force (spring constant 0.3 N/m)

obtained for the film without and with ultrasonic irradiation.

4. Conclusion

It was shown, for the first time, that the electrochemical polymerization of polypyrrole under high frequency sonication was possible on Si substrates. More, thanks to a better mass transfer, the preparation of coatings having the same thickness is quicker in ultrasounds conditions than in silent conditions as proved by chronocoulometry. Then, it was demonstrated that sonoelectrodeposited films are more homogeneous and have a smaller roughness than other polymer films. Moreover, it was shown that the adhesion forces between sonicated polypyrrole films and Si substrates are very weak. This latter result indicates that sonicated polypyrrole films are good candidates for applications in robotics since the micromanipulation of robots needs the reduction and the minimization of the adhesion forces between the micro-objects and the gripper. The influence of the thickness has also been studied. It was demonstrated that the decrease of the thickness, for sonicated polypyrrole

17

films, led to surfaces having smaller roughness and better homogeneity, and above all to a decrease of the adhesion forces. Consequently, the main perspectives of this work consist in the functionalization of micro-objects by thin sonicated polypyrrole films and their applications in micromanipulation task. The possibility to obtain conducting polymers with improved properties (better mass transfer, better homogeneity, small roughness) by the use of sonoelectrochemistry is another original result from this work and also opens new perspectives in the polymer science.

References

[1] S. Shirakawa, E.J. Louis, A.G. MacDiarmid, C.K. Chiang and A.J. Heeger, J. Chem. Soc. Chem. Commun. 578 (1977).

[2] H. Shirakawa, Angew. Chem. Int. Ed. 40 (2001) 2574.

[3] R.K. Sharma, A.C. Rastogi, S.B. Desu, Electrochem. Com. 10 (2008) 268.

[4] J.Wang, C.Y. Wang, C.O. Too, G.G. Wallace, J. Power Sources 161 (2006) 1458.

[5] B.N. Grgur, M.M. Gvozdenovic, J. Stefanovic, B.Z. Jugovic, V.M. Marinovic, Electrochim. Acta 53 (2008) 4627.

18

[6] G. Liang, T. Cui, Solid-State Electronics 48 (2004) 87.

[7] L. Torsi, N. Cioffi, C. Di Franco, L. Sabattini, P.G. Zambonin, T. Bleve-Zacheo, Solid-State Electronics 45 (2001) 1479.

[8] L. Zhao, L. Zhao, Y. Xu, T. Qiu, L. Zhi, G. Shi, Electrochim. Acta 55 (2009) 491.

[9] M. Deepa, S. Ahmad, K.N. Sood, J. Alam, S. Ahmad, A.K. Srivastava, Electrochim. Acta 52 (2007) 7453.

[10] D.M. Lenz, M. Delamar, C.A. Ferreira, J. Electroanal. Chem. 540 (2003) 35.

[11] T. Tücken, B. Yazic, M. Erbil, Materials and Design 28 (2007) 208.

[12] I.L. Lehr, S.B. Saidman, Electrochim. Acta 51 (2006) 3249.

[13] T.A. Bendikov, J. Kim, T.C. Harmon, Sensors Actuators B 106 (2005) 512.

[14] J. Ferreira, E.M. Girotto, Sensors Actuators B 137 (2009) 426.

[15] S. Carquigny, O. Segut, B. Lakard, F. Lallemand, P. Fievet, Synth. Met. 158 (2008) 453.

[16] O. Segut, B. Lakard, G. Herlem, J.Y. Rausch, J.C. Jeannot, L. Robert, B. Fahys, Analytica Chim. Acta 597 (2007) 313.

[17] B. Lakard, O. Segut, S. Lakard, G. Herlem, T. Gharbi, Sensors Actuators B 122 (2007) 101.

[18] B. Lakard, G. Herlem, S. Lakard, R. Guyetant, B. Fahys, Polymer 46 (2005) 12233.

[19] M. Herlem, B. Fahys, G. Herlem, B. Lakard, K. Reybier, A. Trokourey, T. Diaco, S. Zairi, N. Jaffrezic-Renault, Electrochim. Acta 47 (2002) 2597.

[20] B. Lakard, G. Herlem, M. Herlem, A. Etcheberry, J. Morvan, B. Fahys, Surf. Sci. 502-503 (2002) 296.

[21] S. Radhakrishnan, S. Paul, Sensors Actuators B 125 (2007) 60.

[22] V. Vrkoslav, I. Jelinek, G. Broncova, V. Kral, J. Dian, Mat. Sci. Eng. C 26 (2006) 1072.

[23] S. Carquigny, J.B. Sanchez, F. Berger, B. Lakard, F. Lallemand, Talanta 78 (2009) 199.

[24] K. Arora, N. Prabhakar, S. Chand, B.D. Malhotra, Sensors Actuators B 126 (2007) 655.

[25] K. Arora, A. Chaubey, R. Singhal, R.P. Singh, M.K. Pandey, S.B. Samanta, B.D. Malhotra, S. Chand, Biosens. Bioelectron. 21 (2006) 1777.

[26] S.K. Arya, M. Datta, B.D. Malhotra, Biosens. Bioelectron. 23 (2008) 1083.

[27] M.R. Romero, F. Garay, A.M. Baruzzi, Sensors Actuators B 131 (2008) 590.

[28] M. Ates, A.S. Sarac, Progress in Organic Coatings 66 (2009) 337.

[29] M. Zhou, M. Persin, J. Sarrazin, J. Membr. Sci. 117 (1996) 303.

[30] M. Zhou, M. Persin, W. Kujawski, J. Sarrazin, J. Membr. Sci. 108 (1995) 89.

[31] K.H. Xue, C.X. Cai, H. Yang, Y.M. Zhou, S.G. Sun, S.P. Chen, G. Xu, J. Power Sources 75 (1998) 207.

[32] P. Manisankar, A. Gomathi, J. Molecular. Catalysis A 232 (2005) 45.

[33] S. Bereznev, J. Kois, I. Golovtsov, A. Opik, E. Mellikov, Thin Solid Films 511-512 (2006) 425.

[34] M.C. Arenas, H. Hu, J.A. del Rio, A. Sanchez, M.E. Nicho, Solar Energy Mat. Solar Cells 90 (2006) 2413.

[35] G. Wang, H. Chen, H. Zhang, C. Yuan, Z. Lu, G. Wang, W. Yang, Applied Surf. Sci. 135 (1998) 97.

[36] M. Aizawa, H. Shinohara, T. Yamada, K. Akagi, H. Shirakawa, Synth. Met. 18 (1987) 711.

[37] J. Ouyang, Y. Li, Polymer 8 (1997) 1971.

[38] T.F. Otero, I. Cantero, H. Grande, Electrochim. Acta 44 (1999) 2053.

[39] J. Tietje-Girault, C. Ponce de Leon, F.C. Walsh, Surf. Coat. Technol. 201 (2007) 6025.

[40] W. Liang, J. Lei, C.R. Martin, Synth. Met. 52 (1992) 227.

[41] C.O. Yoon, H.K. Sung, J.H. Kim, E. Barsoukov, J.H. Kim, H. Lee, Synth. Met. 99 (1999) 201.

[42] K. West, T. Jacobsen, B. Zachau-Christiansen, M.A. Careem, S. Skaarup, Synth. Met. 55 (1993) 1412.

[43] D.S. Maddison, J. Unsworth, Synth. Met. 30 (1989) 47.

[44] M. Ogamasawara, K. Funahashi, T. Demyra, T. Hagiwara, K. Iwata, Synth. Met. 14 (1986) 61.

[45] S. Maw, E. Smela, K. Yoshida, R.B. Stein, Synth. Met. 155 (2005) 18.

[46] A. Adhikari, S. Radhakrishnan, R. Patil, Synth. Met. 159 (2009) 1682.

[47] G.G. McLeod, K. Jeffreys, J.M.R MacAllister, J. Mundell, S. Affrossman, R.A. Petrick, J. Phys. Chem. Solids 48 (1987) 921.

[48] S. Masubuchi, S. Kazama, R. Matsushita, T. Matsuyama, Synth. Met. 69 (1995) 345.

[49] T. Silk, Q. Hong, J. Tamm, R.G. Compton, Synth. Met. 93 (1998) 59.

[50] M.S. Cho, Y.Y. Yun, J.D. Nam, Y. Son, Y. Lee, Synth. Met. 158 (2008) 1043.

[51] M. Atobe, A Murotani, S. Hitose, Y. Suda, M. Sediko, T. Fuchigami, Al-N. Chowdhury, T. Nonaka, J. Electrochem. Acta, 50 (2004) 977.

[52] M. Atobe, T. Kaburagi, T. Nonakara, D. Kagaku, Electrochemistry 67 (1999) 1114.

[53] M. Atobe, H. Tsuji, R. Asami, T. Fuchigami, J. Electrochem. Soc. 153 (2006) D10.

[54] S. Osawa, M. Ito, K. Tanaka, J. Kuwano, Synth. Met. 18 (1987) 145.

[55] J. Klima, C. Bernard, J. Electroanal. Chem. 462 (1999) 181.

[56] J. Dejeu, P. Rougeot, M. Gauthier, W. Boireau, Micro & Nano Letters 4 (2009) 74.

[57] J. Dejeu, M. Gauthier, P. Rougeot, W. Boireau, ACS Applied Materials & Interfaces, 1 (2009) 1966.

[58] T. Wang, E. Canetta, T.G. Weerakkody, J.L. Keddie, ACS Appl. Mater. Interfaces 1 (2009) 631.

[59] H. Gong, J. Garcia-Turiel, K. Vasilev, O.I. Vinogradova, Langmuir 21 (2005) 7545.

[60] O.I. Vinogradova, G.E. Yakubov, Langmuir 19 (2003) 1227.

[61] E. Charrault, C. Gauthier, P. Marie, R. Schirrer, Langmuir 25 (2009) 5847.

[62] E. Blomberg, E. Poptoshev, P.M. Claesson, F. Caruso, Langmuir 20 (2004) 5432.

[63] A.J. Nolte, J.Y. Chung, M.L. Walker, C.M. Stafford, ACS Appl. Mater. Interfaces 1 (2009) 373.

[64] L. Hallez, F. Touyeras, J-Y. Hihn, J. Klima, Ultrason. Sonochem. 14 (2007) 739

[65] A. Et Taouil, F.Lallemand, J-Y. Hihn, J.M. Melot, V. Blondeau-Patissier, B. Lakard, Ultrason. Sonochem. under press.

[66] A.J. Downard, D. Pletcher, J. Electroanal. Chem. 206 (1986) 139.

[67] F.A. Harraza, J. Electrochem. Soc. 153 (2006) C349.

[68] A.F. Diaz, J.I. Castillo, J.A. Logan, W.J. Lee, J. Electroanal. Chem. 129 (1981) 115.

[69] J.J. Lopez Cascales, T.F. Otero, J. Chem. Phys. 120 (2004) 1951.